Electrochemical investigation on the corrosion of 18%Ni M250 grade maraging steel under welded condition in sulfuric acid medium

Pradeep Kumar and A. Nityananda Shetty

Department of Chemistry, National Institute of Technology Karnataka, Surathkal, Srinivasnagar, Mangalore, Karnataka, India, India PIN – 575025, e-mail: nityashreya@gmail.com

The corrosion behavior of welded maraging steel in sulfuric acid solutions has been studied over a range of acid concentrations and solution temperatures by electrochemical techniques such as Tafel extrapolation and electrochemical impedance spectroscopy. The studies have revealed that the corrosion rate of welded maraging steel increases with the increase in temperature and increase in concentration of sulfuric acid in the medium. The thermodynamic parameters such as activation energy, enthalpy of activation and entropy of activation for the corrosion process are calculated. The results obtained through the two techniques are in good agreement. The surface morphology and surface composition of the corroded samples have been examined by scanning electron microscopy (SEM) and energy-dispersive X-ray (EDX) analysis, respectively.

Keywords: maraging steel, EIS, polarization, SEM, EDX.

УДК 541.138

INTRODUCTION

Corrosion of metals and alloys is a natural process, but its many and varied consequences are considered to be detrimental for the safe, reliable and efficient operation of equipment and structures. Maraging steel, the most extensively used engineering material, gets corroded under many circumstances, especially in some industrial processes, such as acid cleaning, acid descaling and oil well acidizing. An alloy can be a low-carbon steel that traditionally contains about 18 wt % Ni, substantial amounts of Co and Mo together with small additions of Ti. However, depending on the demands of the market, the composition of the material can be modified [1]. For many of the applications of maraging steels, welding is an important means of fabrication. The unique property of being weldable in the solutionized condition followed by a low temperature (480°C) post-weld maraging treatment makes these steels attractive for fabrication of large structures [2]. According to available literature, atmospheric exposure of 18 Ni maraging steel leads to its corrosion in a uniform manner and makes it completely rust covered [3, 4]. Bellanger et al. [5] have reported that the corrosion behavior of maraging steel at the corrosion potential depends on pH and intermediates remaining on the maraging steel surface in the active region favoring the passivity in radioactive water. Maraging steels were found to be less susceptible to hydrogen embrittlement than common high strength steels due to significantly low diffusion of hydrogen in them [6]. But there seems to be no literature available that reveals corrosion behavior of 18% Ni M250 grade maraging steel under welded condition in acid medium. So, the corrosion behavior of welded maraging steel in sulphuric acid medium is in the focus of the study in the present paper.

EXPERIMENTAL

Material

The experiments were performed with a specimen of the welded maraging steel (18% Ni M250 grade). Percentage composition of 18% Ni M250 grade maraging steel sample is given in Table 1. The maraging steel was welded by GTAW-DCSP, with 5 passes using filler material of composition as given in Table 2. The working electrode was in the form of a rod machined into a cylindrical form embedded in epoxy resin leaving an open surface area of 0.6458 cm^2. This coupon was abraded as per standard metallographic practice, belt grinding followed by polishing on emery papers of grade 600, 800, 1000, 1200, 1500, 2000, and finally on polishing wheel using legated alumina abrasive to obtain mirror finish degreased with acetone and dried before immersing in the medium.

Electrolytes

Analytical grade of sulfuric acid and doubly distilled water were used for preparing the test solutions having concentrations 0.1M, 0.5M, 1M, 1.5M and 2M. Analyses were carried out in a calibrated thermostat at temperatures 30°C, 40°C, 50°C and 60°C (±0.5°C).

Table 1. Composition of the specimen (% by weight)

Element	Composition	Element	Composition
C	0.015%	Ti	0.3–0.6%
Ni	17–19%	Al	0.005–0.15%
Mo	4.6–5.2%	Mn	0.1%
Co	7–8.5%	P	0.01%
Si	0.1%	S	0.01%
O	30 ppm	N	30 ppm
H	2.0 ppm	Fe	Balance

Table 2. Composition of the filler material used for welding (% by weight)

Element	Composition	Element	Composition
C	0.015%	Ti	0.015%
Ni	17%	Al	0.4%
Mo	2.55%	Mn	0.1%
Co	12%	Si	0.1%
Fe	Balance		

Electrochemical measurements

Electrochemical experiments were performed in a conventional three-electrode system by using an electrochemical work station Gill AC having ACM instrument Version 5 software. The measurements were carried out using a conventional three electrode Pyrex glass cell with platinum foil as the counter electrode and a saturated calomel electrode as the reference electrode. The sample specimen was used as the working electrode.

Tafel polarization studies

A finely polished welded maraging steel specimen, sealed by epoxy resin with the exposure surface of 0.6458 cm^2 (the working electrode) was exposed to the corrosion medium with different concentrations of sulfuric acid (0.1M to 2.0M), at different temperatures (30°C to 60°C), and allowed to establish a steady state open circuit potential. The potentiodynamic current – potential curves were recorded by polarizing the specimen to -250 mV cathodically and +250 mV anodically with respect to the open circuit potential (OCP) at a scan rate of 1 mV s^{-1}.

Electrochemical impedance spectroscopy studies

Electrochemical impedance spectroscopy (EIS), which gives early information about the electrochemical processe at the metal solution interface, was applied in many corrosion studies as reported in [7]. EIS measurements were carried out on the steady open circuit potential (OCP) disturbed with amplitude of 10 mV a.c. sine wave at frequencies from 100 KHz to 10 mHz. Impedance data were analyzed using Nyquist plots. The charge transfer resistance, R_{ct} was extracted from the diameter of the semicircle in the Nyquist plot.

In all of the above measurements, at least three similar results were considered and their average values were given in [7].

The scanning electron microscope images were recorded to establish the interaction of acid medium with the metal surface using JEOL JSM-6380LA analytical scanning electron microscope.

RESULTS AND DISCUSSION

Tafel polarization measurements

The effect of sulfuric acid concentration and solution temperature on the corrosion rate of welded samples of maraging steel was studied using Tafel polarization technique. The anodic and cathodic current-potential curves are extrapolated up to their intersection at the point where corrosion current density (i_{corr}) and corrosion potential (E_{corr}) are obtained [8]. The potentiodynamic polarization curves for the corrosion of welded maraging steel in different concentrations of H_2SO_4 at 50°C are shown in Fig. 1. As is seen there, the polarization curves are shifted to the high current density region as the concentration of H_2SO_4 increases, indicating the increase in the corrosion rate with the increase in the concentration of H_2SO_4. The potentiodynamic polarization parameters such as corrosion potential (E_{corr}), corrosion current (i_{corr}), anodic and cathodic slopes (b_a and b_c) and corrosion rate (υ_{corr}) are calculated from the Tafel plots and are listed in Table 3.

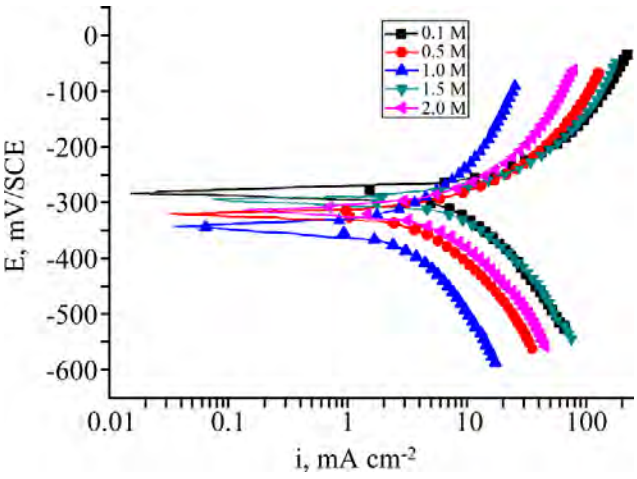

Fig. 1. Potentiodynamic polarization curves for the corrosion of welded maraging steel in different concentrations of H_2SO_4 at 50°C.

The corrosion rate is calculated using Eq. 1 below:

$$\upsilon_{corr}(mmy^{-1}) = \frac{3270 \times M \times i_{corr}}{\rho \times Z} \quad (1)$$

Table 3. Electrochemical polarization parameters for the corrosion of welded maraging steel in different concentrations of H_2SO_4 at different temperatures

Molarity of H_2SO_4 (M)	Temperature (K)	Corrosion potential (mV vs SCE)	Anodic slope (mV dec^{-1})	Cathodic slope (mV dec^{-1})	Corrosion current (mA cm^{-2})	Corrosion rate (mm y^{-1})
0.1	303	–356	240	–146	1.98	25.52
	313	–347	248	–156	2.93	37.76
	323	–323	342	–349	6.14	79.14
	333	–337	321	–245	9.38	120.91
0.5	303	–322	312	–154	2.47	31.84
	313	–318	261	–225	4.71	60.71
	323	–312	329	–204	6.94	90.02
	333	–308	380	–208	10.45	134.29
1.0	303	–315	233	–84	3.07	39.57
	313	–310	314	–186	4.96	63.93
	323	–319	369	–241	8.71	112.17
	333	–314	327	–232	12.81	164.02
1.5	303	–313	386	–170	3.38	43.43
	313	–300	335	–179	5.63	72.57
	323	–295	376	–255	9.73	127.56
	333	–303	375	–250	15.61	200.34
2.0	303	–293	335	–167	3.72	47.95
	313	–290	367	–204	6.38	82.24
	323	–283	410	–280	11.27	148.41
	333	–276	418	–271	18.02	232.76

where 3270 is the constant that defines the unit of the corrosion rate, i_{corr} is the corrosion current density in A cm^{-2}, ρ is the density of the corroding material, 8100 kg m^{-3}, M is the atomic mass of the metal, and Z is the number of electrons transferred per metal atom [9].

From the data summarized in Table 3 it is clear that the corrosion rate of the welded maraging steel specimen increases with an increase in the strength of sulfuric acid in the solution. It is also deduced from the results that the corrosion potential is shifted towards less negative values as the concentration of sulfuric acid increases.

The corrosion of steel normally proceeds via two partial reactions in acid solutions. The partial anodic reaction involves the oxidation of metal and formation of soluble Fe^{2+} ions, while the partial cathodic reaction involves the evolution of hydrogen gas [10]:

$$\mathrm{Fe} \rightarrow \mathrm{Fe}^{2+} + 2e^{-} \quad \text{(Oxidation)} \qquad (2)$$

$$2\mathrm{H}^{+} + 2e^{-} \rightarrow \mathrm{H}_2 \uparrow \quad \text{(Reduction)} \qquad (3)$$

The overall chemical reaction can be expressed as follows [11]:

$$\mathrm{Fe} + \mathrm{H_2SO_4} \rightarrow \mathrm{FeSO_4} + \mathrm{H_2} \uparrow \qquad (4)$$

Although the overall corrosion rate of the welded maraging steel in concentrated sulfuric acid is low, still some corrosion procedes. The reaction products of the corrosion process are iron sulfate and hydrogen gas.

Electrochemical impedance spectroscopy

The corrosion behavior of the welded maraging steel was also investigated by EIS with different concentrations of sulfuric acid at different temperatures. The Nyquists plots for the corrosion of the welded maraging steel in sulfuric acid solutions of different concentrations at 50°C are shown in Fig. 2. The point where the semicircle of the Nyquist plot intersects the real axis at high frequency (close to the origin) yields the solution resistance (R_s). The intercept on the real axis at the other end of the semicircle (low frequency) gives the sum of the solution resistance and the charge transfer resistance (R_{ct}). Hence the charge transfer resistance value is simply the diameter of the semicircle [12]. The diagonal region in between the high frequency and low frequency regions has a negative slope due to the capacitive behavior of the electrochemical double layer.

The corrosion current density is calculated using the Stern Geary Equation 5 as in [13]:

$$i_{corr} = \frac{b_a b_c}{2.303(b_a + b_c)R_{ct}}. \qquad (5)$$

Figure 2 demonstrates that the diameter of the semicircle decreases with the increase in the concentration of H_2SO_4, thus indicating the decrease in R_{ct} value

and the increase in the corrosion rate. The fact that impedance diagrams have semicircular appearance indicates that the corrosion of the welded maraging steel is controlled by a charge transfer process and the mechanism of dissolution of metal in H_2SO_4 is not altered with the change in the H_2SO_4 concentration [14]. Also Fig. 2 shows the Nyquist plots as not perfect semicircles. The deviation has been attributed to frequency dispersion. The "depressed" semicircles have a center under the real axis and can be seen as depressed capacitive loops. Such phenomena often correspond to surface heterogeneity, which may be the result of surface roughness, dislocations, distribution of the active sites or adsorption of molecules [15].

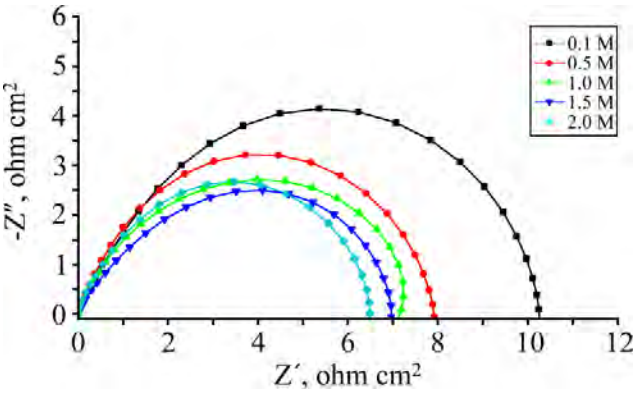

Fig. 2. Nyquist plots for the corrosion of welded maraging steel in different concentrations of H_2SO_4 at 50°C.

The results obtained can be interpreted in terms of the equivalent circuit of the electrical double layer as shown in Fig. 3. The circuit fitment was done by ZSimpWin software of version 3.21. The equivalent circuit consists of solution resistance R_s, *the* charge transfer resistance R_{ct} and a constant phase element $(CPE)_l$ parallel to R_{ct}. The constant phase element (Q_{dl}) is substituted for the capacitive element to give a more accurate fit, as most capacitive loops are depressed semicircles rather than regular semicircles [16].

The impedance of the constant phase is given by the expression:

$$Z_Q = Y_0^{-1}(j\omega)^{-n} \tag{6}$$

where Y_0 is the proportional factor, n has the meaning of a phase shift, and $j = (-1)^{1/2}$. The value of the double layer capacitance (C_{dl}) can be obtained from the following equation:

$$C_{dl} = Y_0(\omega_m^n)^{n-1} \tag{7}$$

where ω_m^n is the frequency at which the imaginary part of the impedance has maximum [16].

The results of EIS measurement are summarized in Table 4. They show that the charge transfer resistance (R_{ct}) value decreases and the double layer capacitance (C_{dl}) increases with the increase in the concentration of sulfuric acid. The Nyquist plots obtained in the real system represent general behavior where the double layer on the interface of metal/solution does not behave as a real capacitor. On the metal side, electrons control the charge distribution whereas on the solution side it is controlled by ions. As ions are much larger than electrons, the equivalent ions to the charge on the metal will occupy quite a large volume on the solution side of the double layer. Increase in the capacitance, which can result from an increase in the local dielectric constant and/or a decrease in the thickness of the electrical double layer, suggests that the sulfate ions act by adsorption at the metal/solution interface [17].

Effect of temperature

The effect of temperature on the corrosion rate of the welded maraging steel was studied by measuring the corrosion rate at the temperature range of 30°C–60°C. Figs. 4 and 5 represent the potentiodynamic polarization curves and Nyquist plots, respectively, at different temperatures for the corrosion of welded maraging steel sample in 1M H_2SO_4 solution. Similar plots were obtained in other concentrations of solutions also. The Tafel polarization results and EIS results at different temperatures are listed in Tables 3 and 4, respectively. From Figs 4 and 5 and from the results in Tables 3 and 4 it is evident that the corrosion rate increases with the increase in temperature. This may be attributed to the fact that the hydrogen evolution overpotential decreases with the increase in temperature that leads to an increase in cathodic reaction rate [18]. The values of b_c and b_a change with the increase in acid concentration and also with the increase in temperature, which indicates the influence of acid concentration and temperature on the kinetics of both hydrogen evolution and metal dissolution.

Activation energy (E_a) for the corrosion process of the welded maraging steel in sulfuric acid was calculated from the Arrhenius equation (Eq. 8) as in [3, 4]:

$$\ln \upsilon_{corr} = B - \frac{E_a}{RT} \tag{8}$$

where B is a constant that depends on the metal type, and R is the universal gas constant. The plot of ln (υ_{corr}) versus reciprocal of absolute temperature ($1/T$) gives a straight line with the slope = $-E_a/R$, from which the activation energy values for the corrosion process were calculated. The Arrhenius plots for the welded specimen are shown in Fig. 6.

The enthalpy and entropy of activation ($\Delta H^{\#}$ & $\Delta S^{\#}$) were calculated from the transition state theory (see Eq. 9 as in [19]):

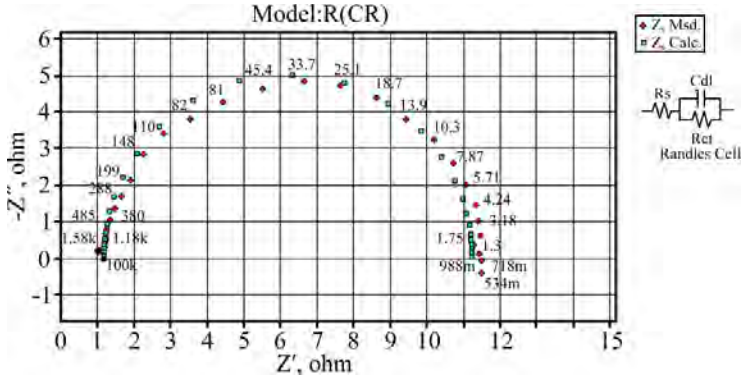

Fig. 3. Equivalent circuit model used to fit the experimental data for the corrosion of Welded maraging steel in 0.1M H_2SO_4 solution at 50°C.

Table 4. Impedance parameters for the corrosion of welded maraging steel in different concentrations of H_2SO_4 at different temperatures

Molarity of H_2SO_4 (M)	Temperature (K)	Charge transfer resistance (Ω cm^2)	Double layer capacitance (μF cm^{-2})	Corrosion rate (mm y^{-1})
0.1	303	20.12	1327.0	25.26
	313	14.11	1341.0	38.03
	323	10.24	1513.0	78.11
	333	6.53	1833.0	119.10
0.5	303	18.73	1320.0	30.81
	313	11.41	1358.0	59.29
	323	7.90	1396.0	89.09
	333	5.39	1635.0	131.41
1.0	303	16.01	679.9	38.02
	313	10.34	677.7	62.77
	323	7.28	571.0	108.17
	333	4.34	1162.0	158.32
1.5	303	15.93	962.2	41.37
	313	9.37	902.2	69.61
	323	6.94	788.8	124.38
	333	4.16	764.1	193.25
2.0	303	13.87	562.0	44.89
	313	9.17	482.0	80.05
	323	6.48	622.5	143.16
	333	4.03	781.6	226.32

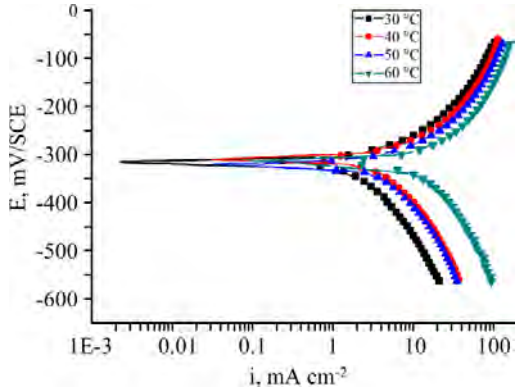

Fig. 4. Potentiodynamic polarization curves for the corrosion of welded maraging steel in 1M H_2SO_4 at different temperatures.

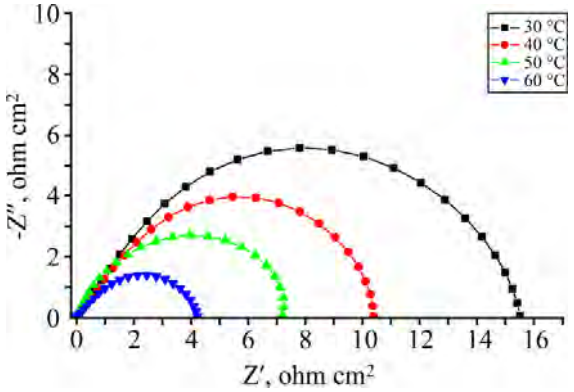

Fig. 5. Nyquist plots for the corrosion of welded maraging steel in 1M H_2SO_4 at different temperatures.

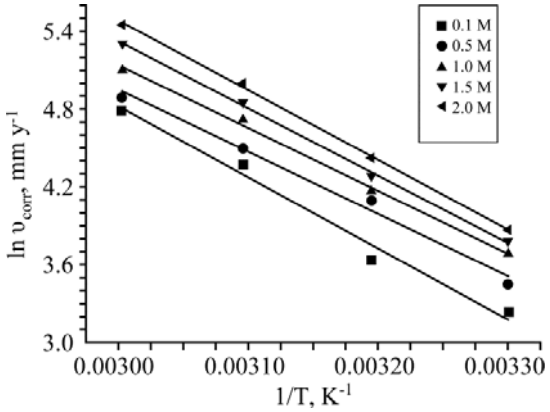

Fig. 6. Arrhenius plots for the corrosion of welded maraging steel in H_2SO_4.

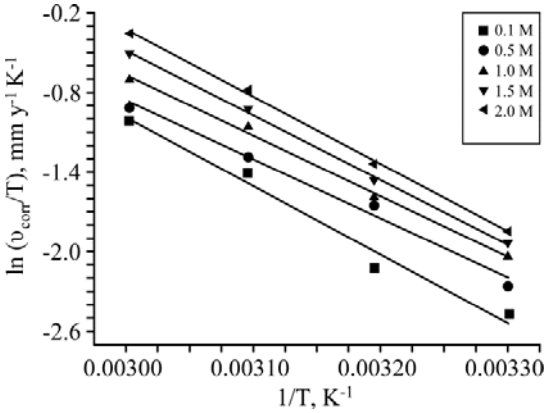

Fig. 7. Plots of $\ln(\upsilon_{corr}/T)$vs$1/T$ for the corrosion of welded maraging steel in H_2SO_4.

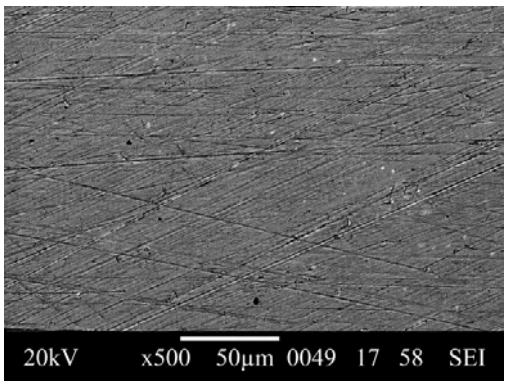

(a)

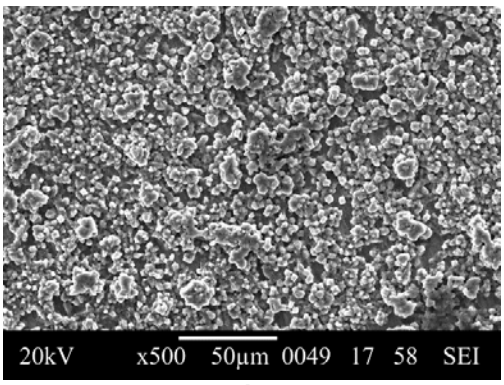

(b)

Fig. 8. SEM images of (a) freshly polished surface, (b) corroded surface.

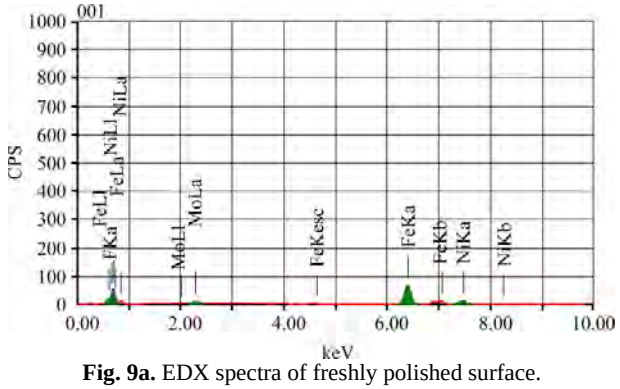

Fig. 9a. EDX spectra of freshly polished surface.

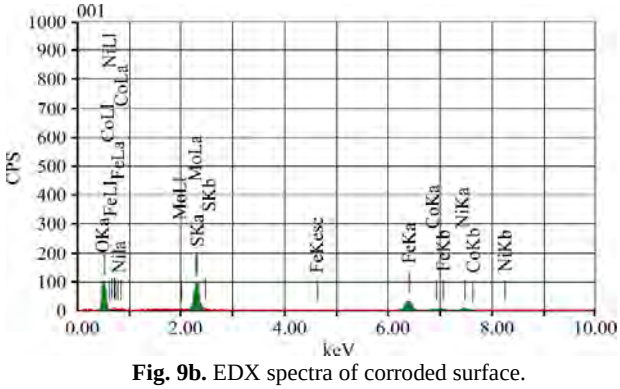

Fig. 9b. EDX spectra of corroded surface.

$$\upsilon_{corr} = \frac{RT}{Nh} e^{\frac{\Delta S^{\#}}{R}} e^{\frac{-\Delta H^{\#}}{RT}} \qquad (9)$$

where h is Planck's constant, N is Avogadro's number and R is the ideal gas constant. A plot of $\ln(\upsilon_{corr}/T)$ versus $1/T$ gives a straight line with the slope = $-\Delta H^{\#}/R$ and intercept = $\ln(R/Nh) + \Delta S^{\#}/R$. The plots of $\ln(\upsilon_{corr}/T)$ versus $1/T$ for the corrosion of the welded maraging steel in different concentrations of sulfuric acid are depicted in Fig. 7.

Table 5. Activation parameters for the corrosion of welded maraging steel in sulfuric acid

Molarity of H_2SO_4 (M)	Energy of activation (kJ mol^{-1})	Enthalpy of activation (kJ mol^{-1})	Entropy of activation (J K^{-1} mol^{-1})
0.1	43	46	-21
0.5	37	40	-37
1.0	38	39	-34
1.5	41	43	-24
2.0	42	45	-18

The activation parameters calculated are listed in Table 5. The activation energy values indicate that the corrosion of the alloy is controlled by the surface reaction, since the values of the activation energy for the corrosion process exceed 20 kJ mol^{-1} [20]. The entropy of activation is negative. This implies that the activated complex in the rate-determining step represents association rather than dissociation, indicating that a decrease in randomness takes place when going from reactants to the activated complex [17].

SEM and EDX examinations of the electrode surface

The SEM images were recorded to establish the interaction of the acid solution with the metal surface. The SEM image of a freshly polished surface of the welded maraging steel sample (Fig. 8a) shows the uncorroded surface with few scratches due to polishing. Fig. 8b shows the SEM image of the welded maraging steel surface after being immersed for 3 h in 2.0 M H_2SO_4. The SEM images demonstrate that the specimen without being immersed in the acid solutions is in a better condition having a smooth surface, while the metal surface immersed in 2.0 M H_2SO_4 is deteriorated due to the acid action. The corroded surface shows detachment of particles from the surface.

EDX survey spectra were used to determine the surface composition of the specimen before and after the exposure to the acid solution. Fig. 9a reveals the fresh surface of the specimen with an intense peak of Fe. The spectrum in Fig. 9b shows that the Fe peaks are considerably suppressed relative to the fresh specimen; and new peaks have appeared for oxygen and sulfur. The suppression of the Fe lines indicates that the specimen has undergone corrosion in the presence of sulfuric acid. The presence of sulfur and oxygen peaks indicate the presence of sulfate ion on the surface the corrosive medium and this could be due to the formation of $FeSO_4$ during corrosion.

CONCLUSIONS

From the above results and discussion, the main conclusions can be summarized in the following points:

1. The corrosion rate of the welded maraging steel specimen in sulfuric acid medium is quite high.

2. The corrosion rate is influenced by temperature and concentration of sulfuric acid medium. The corrosion rate of the specimen under investigation increases with the increase in solution temperature and in the concentration of sulfuric acid.

3. The corrosion kinetics follows the Arrhenius law.

4. The results obtained from the Tafel polarization curves and electrochemical impedance spectroscopies are in good agreement.

REFERENCES

1. Stiller K., Danoix F., Bostel A. Investigation of Precipitation in a New Maraging Stainless Steel. *Applied Surface Science.* 1996, **94/95**, 326–333.
2. Adama C.M., Travis R.E. Welding of 18% Ni-Co-Mo Maraging Alloys. *Welding Journal*. 1964, **43**, 193–197.
3. Poornima T., Nayak J., Shetty A.N. Corrosion of Aged and Annealed 18 Ni 250 Grade Maraging Steel in Phosphoric Acid Medium, *International Journal of Electrochemical Science*. 2010, **5**, 56–71.
4. Poornima T., Nayak J., Shetty A.N. 3,4-Dimethoxy Benzaldehyde Thiosemicarbazone as Corrosion Inhibitor for Aged 18Ni 250 Grade Maraging Steel in 0.5 M Sulfuric Acid. *Journal of Applied Electrochemistry.* 2011, **41**, 223–233.
5. Bellanger G., Rameau J.J. Effect of Slightly Acid pH with or without Chloride in Radioactive Water on the Corrosion of Maraging Steel. *Journal of Nuclear Materials*. 1996, **228**, 24–37.
6. Rezek J., Klein I. E., Yhalom J. Electrochemical Properties of Protective Coatings on Maraging Steel. *Corrosion Science*. 1997, **39**, 385–391.
7. Bellanger G. Effect of Carbonate in Slightly Alkaline Medium on the Corrosion of Maraging Steel. *Journal of Nuclear Materials.* 1994, **217**, 187–193.
8. Khaled K. The Inhibition of Benzimidazole Derivatives on Corrosion of Iron in 1M HCl Solutions. *Electrochim. Acta*. 2003, **48**, 2493–2498.
9. Fontana M.G. *Corrosion Engineering*, 3rd ed. McGraw Hill, Singapore, 1987.
10. Kriaa A., Hamdi N., Jbali K., Tzimann M. Corrosion of Iron in Highly Acidic Hydro-organic Solutions. *Corrosion Science*. 2009, **51**, 668–676.
11. Amin A.M., Khaled K.F., Mohsen Q. A Study of the Inhibition of Iron Corrosion in HCl Solutions by Some Amino Acids. *Corrosion Science.* 2010, **52**, 1684–1695.
12. Prabhu R.A., Venkatesha T.V., Shanbhag A.V., Kulkarni G.M., Kalkhambkar R.G. Inhibition Effects of some Schiff's Bases on the Corrosion of Mild Steel in Hydrochloric Acid Solution. *Corrosion Science*. 2008, **50**, 3356–3362.
13. El-Sayed A. Phenothiazine as Inhibitor of the Corrosion of Cadmium in Acidic Solutions. *Journal of Applied Electrochemistry*. 1997, **27**, 89–94.
14. Larabi L., Harek Y., Traisnel M., Mansri A. Inhibition of the Corrosion of Iron by Oxygen and Nitrogen Containing Compounds. *Journal of Applied Electrochemistry*. 2004, **34**, 833–839.
15. Li W.H., He Q., Zhang S.T., Pei C.L., Hou B.R. Some New Triazole Derivatives as Inhibitors for Mild Steel

Corrosion in Acidic Medium. *Journal of Applied Electrochemistry*. 2008, **38**, 289–295.

16. Tang Y., Chen Y., Yang W. Electrochemical and Theoretical Studies of Thienyl-substituted Amino Triazoles on Corrosion Inhibition of Copper in 0.5 M H_2SO_4. *Journal of Applied Electrochemistry*. 2008, **38**, 1553–1559.
17. Prabhu R.A., Shanbhag A.V., Venkatesha T.V. Influence of Tramadol [2-[(dimethylamino)methyl]-1-(3-methoxyphenyl) Cyclohexanol Hydrate] on Corrosion Inhibition of Mild Steel in Acidic Media. *Journal of Applied Electrochemistry*. 2007, **37**, 491–497.
18. Larabi L., Harek Y., Benali O., Ghalem S. Hydrazide Derivatives as Corrosion Inhibitors for Mildsteel in 1M HCl. *Progress in Organic Coatings*. 2005, **54**, 256–262.
19. Abdi EI-Rehim S.S., Ibrahim M.A.M., Khaled K.F. 4-Aminoantipyrine as an Inhibitor of Mild Steel Corrosion in HCl Solution. *Journal of Applied Electrochemistry*, 1999, **29**, 593–599.
20. Bouklah M., Hammouti B., Benkaddour M., Benhadda T. Thiophene Derivatives as Effective Inhibitors for the Corrosion of Steel in 0.5 M H_2SO_4. *Journal of Applied Electrochemistry*. 2005, **35**, 1095–1101.

Received 28.05.12
Accepted 27.06.12

Реферат

Коррозийное поведение сварной мартенситностареющей стали в растворах серной кислоты было изучено при различных концентрациях кислоты и температурах раствора с помощью таких электрохимических методов, как экстраполяция Тафеля и электрохимический импеданс спектроскопии. Исследование показало, что скорость коррозии сварной мартенситностареющей стали возрастает с увеличением температуры и концентрации серной кислоты в среде. Были рассчитаны такие термодинамические параметры, как активирующая энергия, энтальпия активации и энтропия активации для коррозионных процессов. Результаты, полученные при применении обоих методов, находятся в хорошем согласии. Морфология и состав поверхности корродированных образцов были изучены с помощью сканирующей электронной микроскопии (SEM) и энергодисперсионным рентгеновским анализом (EDX).

Ключевые слова: мартенситностареющая сталь, EIS, поляризация, SEM, EDX .